ISCI, Volume *15*

Supplemental Information

Necroptosis of Intestinal Epithelial Cells Induces Type 3 Innate Lymphoid Cell-Dependent Lethal Ileitis

Ryodai Shindo, Masaki Ohmuraya, Sachiko Komazawa-Sakon, Sanae Miyake, Yutaka Deguchi, Soh Yamazaki, Takashi Nishina, Takayuki Yoshimoto, Soichiro Kakuta, Masato Koike, Yasuo Uchiyama, Hiroyuki Konishi, Hiroshi Kiyama, Tetuo Mikami, Kenta Moriwaki, Kimi Araki, and Hiroyasu Nakano

ShindoFigS1

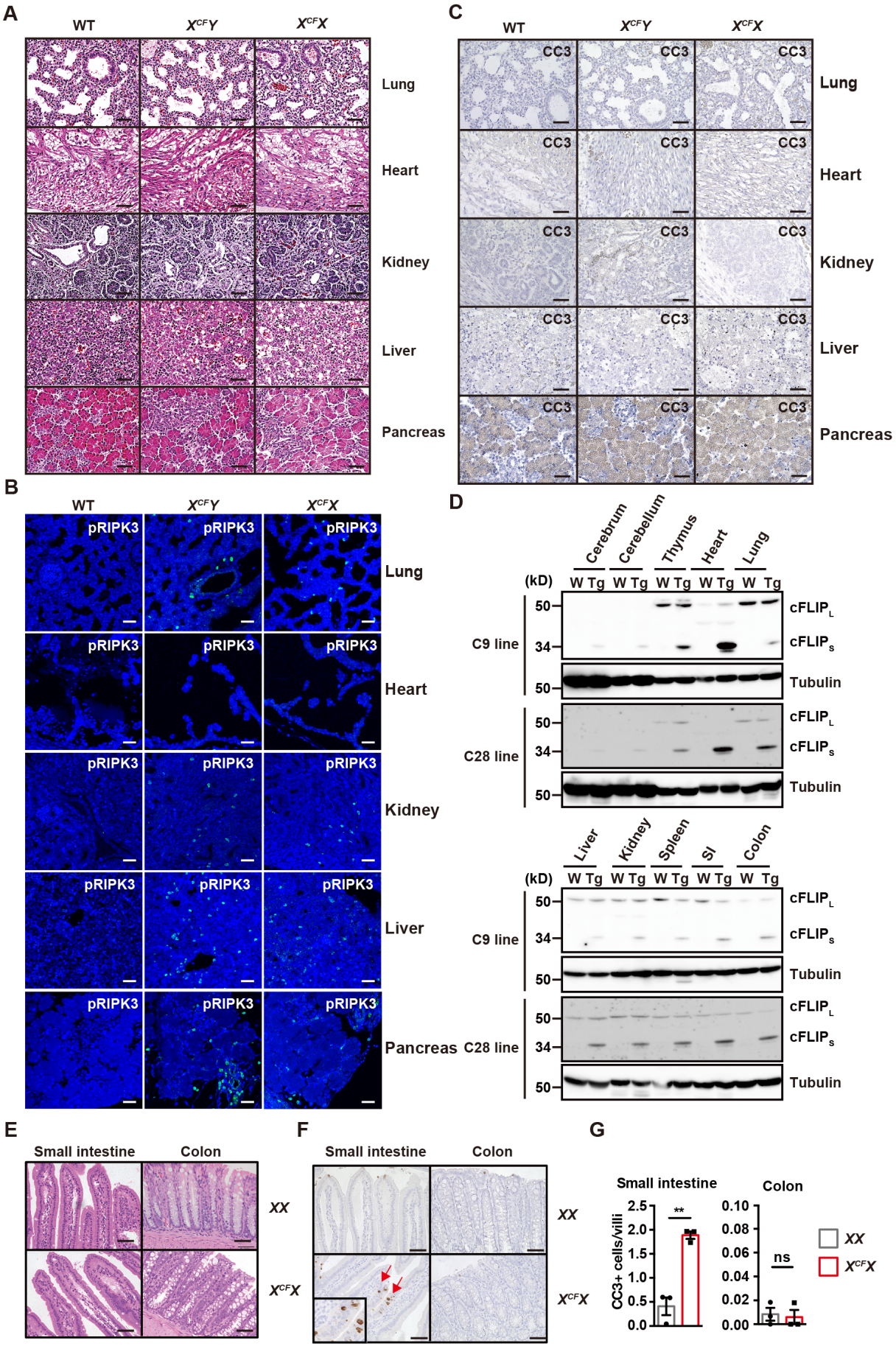

Figure S1. pRIPK3-, but not CC3-positive cells are detected in various tissues of *CFLARs* Tg mice, Related to Figure 1.

(A-C) Tissue sections from mice of the indicated genotypes at E18.5 were stained with H&E (A), anti-pRIPK3 (B), or anti-CC3 (C) antibodies (n=3 to 5 mice per each genotype). The tyramide signal amplification (TSA) method was used to enhance pRIPK3-positive signals. Scale bars, 50 μm.

(D) The expression of endogenous $cFLIP_L$ and exogenously introduced human cFLIPs in various tissues of 8-week-old $X^{CF}X$ mice. Extracts were prepared from various tissues and analyzed by immunoblotting with anti-cFLIP and anti-tubulin antibodies. C9 and C28 indicate two independently generated Tg lines. Results are representative of three independent experiments. W and Tg indicate WT and *CFLARs* Tg mice, respectively.

(E-G) Small numbers of IECs still undergo apoptosis in the SI of adult $X^{CF}X$ mice. Tissue sections of 6- to 8-week-old *XX* and $X^{CF}X$ mice were stained with H&E (E) or anti-CC3 antibody (F) (n= 3 to 5 mice per each genotype). The black box is an enlarged image of $CC3^+$ cells. $CC3^+$ cells are indicated by red arrows. Numbers of $CC3^+$ cells in the small intestine or colon were calculated in randomly selected fields (G). Results are expressed as numbers of $CC3^+$ cells per villi. Results are mean ± SEM (n=3 mice per each genotype). Statistical significance was determined by the two-tailed unpaired Student's *t* test. $^{**}P<0.01$; ns, not significant.

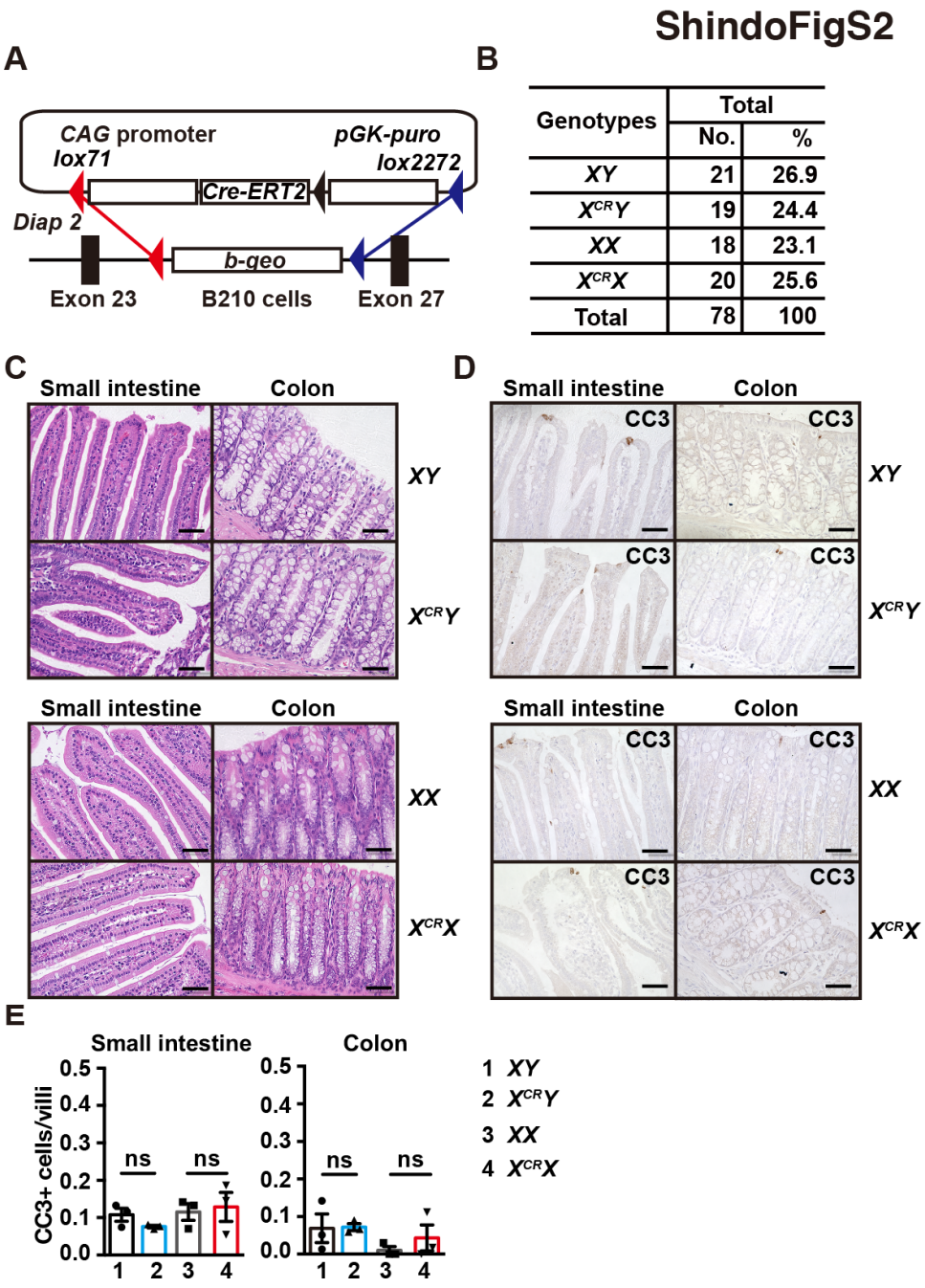

Figure S2. Inactivation of one allele of *Diap2* loci does not induce perinatal lethality, Related to Figure 1.

(A) Diagram of a vector for *Cre-ERT2* Tg mice.

(B) $X^{CR}Y$ mice are born at the expected Mendelian ratio and develop normally. The progeny of crossing male wild-type mice with $X^{CR}X$ mice. The genotypes of 2- to 4-week-old mice were determined by PCR.

(C-E) Small intestinal or colon sections of mice of the indicated genotypes at E18.5 were stained with H&E (C) (n=10 mice per each genotype) or anti-CC3 antibody (D) (n=3 to 4 mice per each genotype). Scale bars, 100 μm. Numbers of $CC3^+$ cells were counted and are expressed as in Figure S1G (E). Results are mean ± SEM (n=3 mice per group). Statistical significance was determined by the two-tailed unpaired Student's *t* test. ns, not significant.

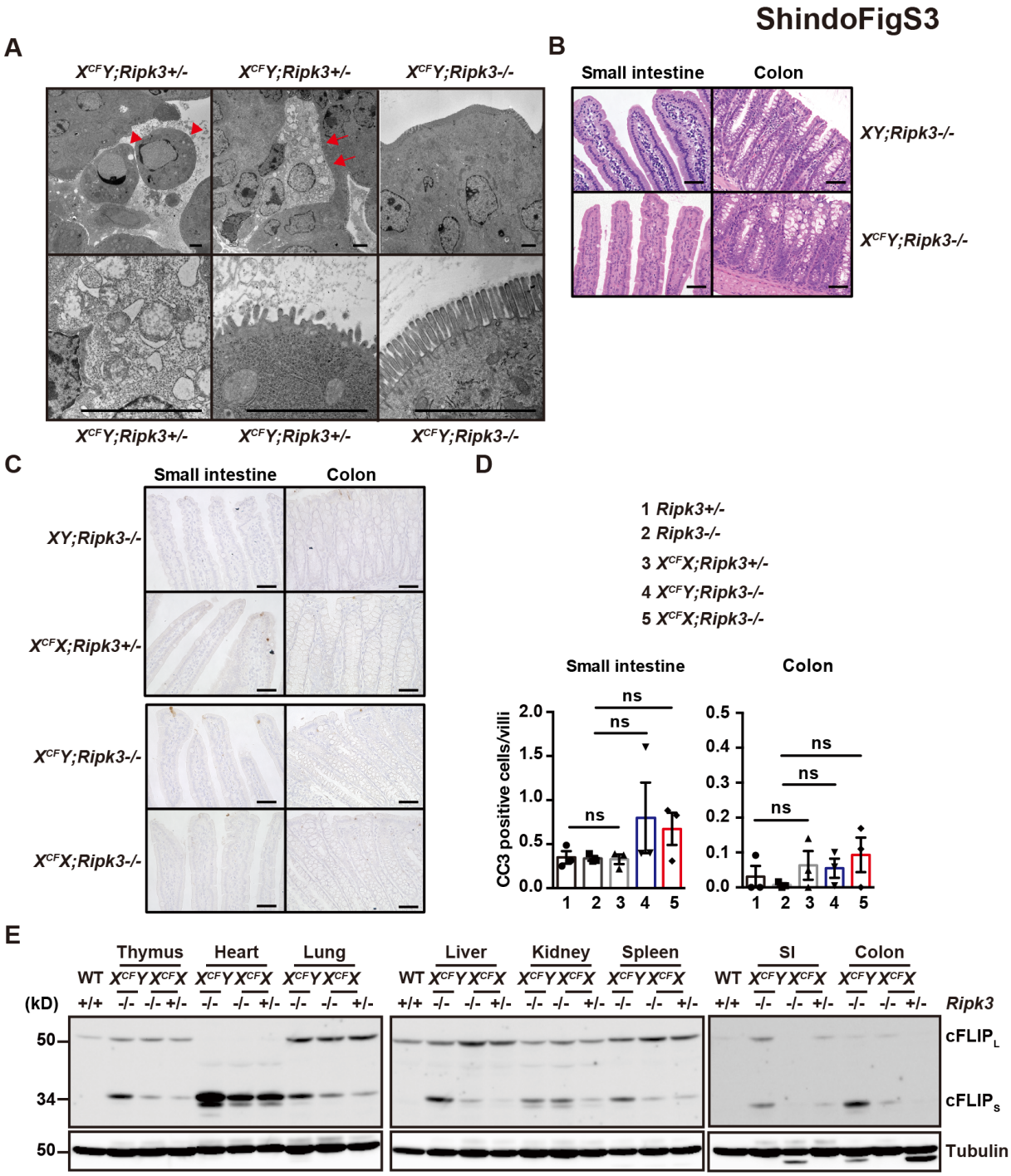

Figure S3. Male *CFLARs* Tg;*Ripk3*-/- mice grow without apparent abnormality, Related to Figure 3.

(A) Transmission electron microscopic analysis of the SI of mice of the indicated genotypes at E18.5. Results are representative of two independent experiments. Scale bars, 5 μm. Red arrowheads and arrows indicate apoptotic and necroptotic cells, respectively.

(B-D) Small intestinal sections from 6- to 8-week-old mice of the indicated genotypes were stained with H&E (B) or anti-CC3 antibody (C) (n= 3 mice per each genotype). Scale bars, 100 μm. Numbers of $CC3^{+}$ cells were counted and are expressed as in Figure S1G (D). Results are mean ± SEM (n=3 mice

per each genotype). Statistical analysis was determined by the one-way ANOVA test. ns, not significant.

(E) Expression of cFLIPs in various tissues. Tissue extracts from mice of the indicated genotype were analyzed by immunoblotting with anti-cFLIP and anti-tubulin antibodies. Results are representative of two independent experiments.

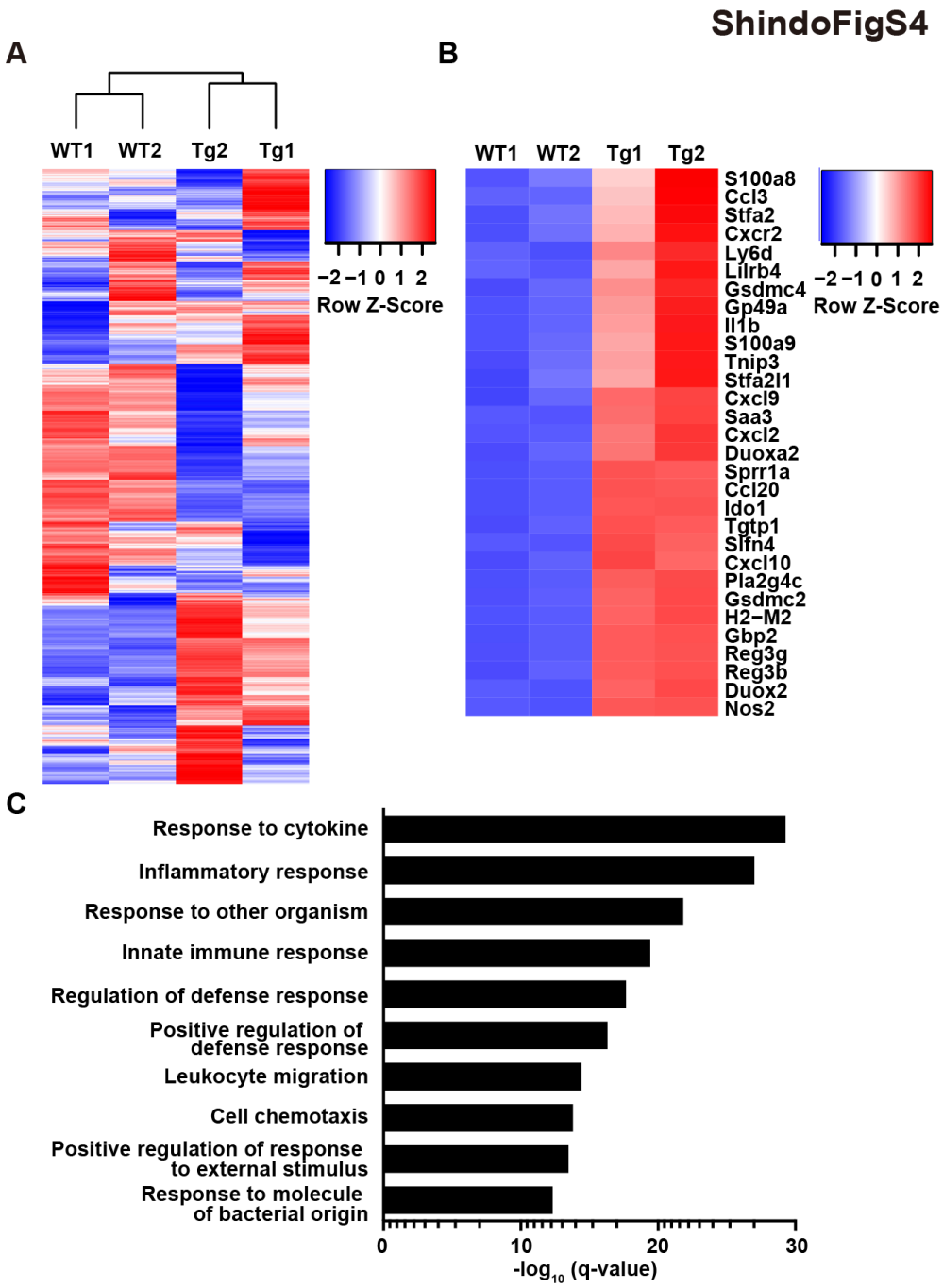

Figure S4. Transcriptome analysis of the SI of *CFLARs* Tg mice, Related to Figure 5.

(A) RNAs were prepared from the SI of mice of the indicated genotype at E18.5, and the expression of genes was determined by microarray analysis. Heat map of microarray gene expression of the SI of the indicated mice and their clustering are shown. Gene-expression color normalized by Z score transformation is shown at the right.

(B) Heat map of 30 genes upregulated more than two-fold in *CFLARs* Tg mice compared to WT mice. Red and blue indicate higher and lower relative expression, respectively.

(C) Signaling pathways significantly enriched in the SI of *CFLARs* Tg mice compared to wild-type mice.

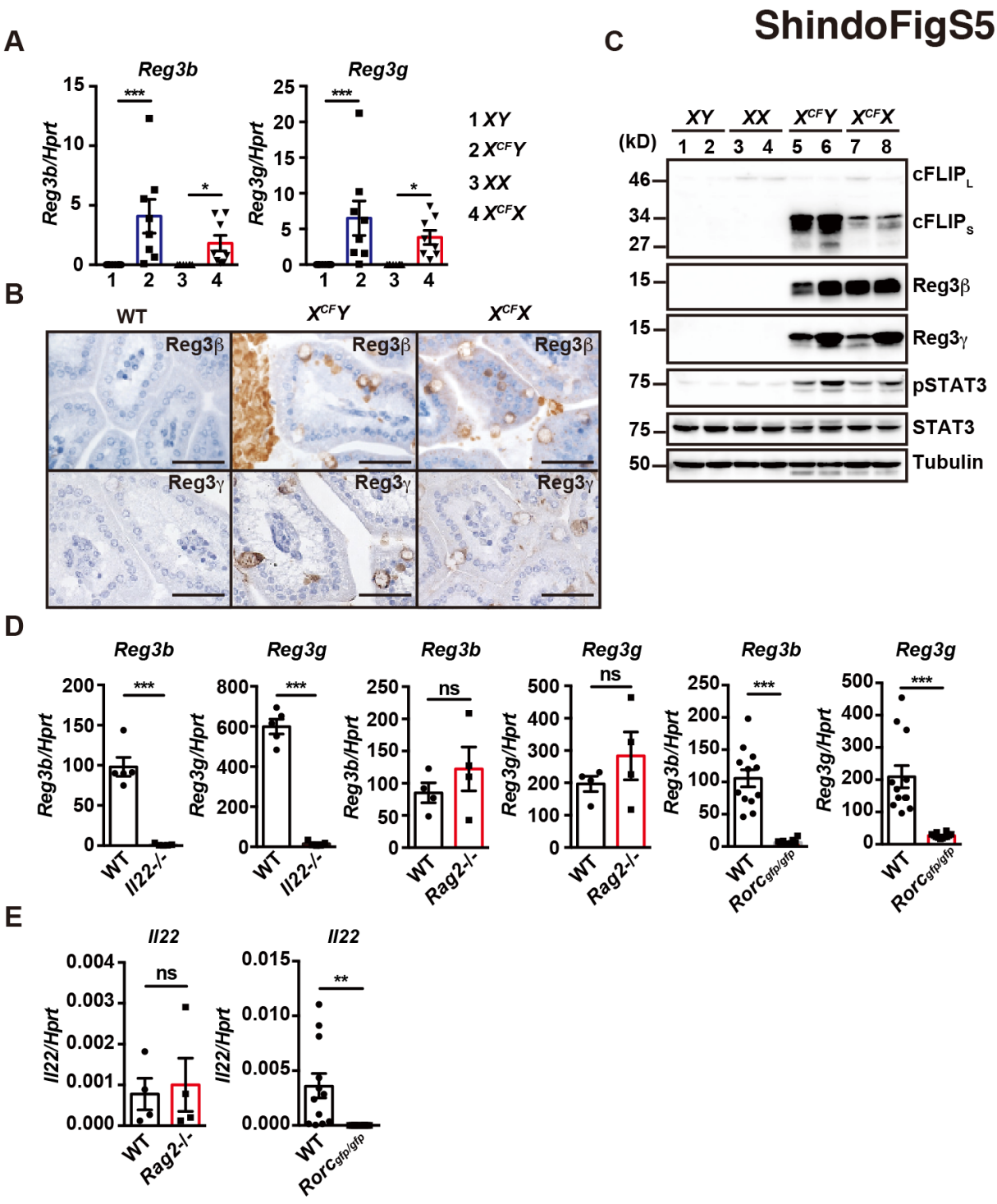

Figure S5. Expression of *Reg3b* and *Reg3g* is elevated in the SI of *CFLARs* Tg mice, Related to Figure 5.

(A) mRNAs were extracted from the SI of mice of the indicated genotypes at E18.5, and the expression of *Reg3b* and *Reg3g* were determined by qPCR. Results are mean ± SEM (n=8 mice per each genotype). Statistical significance was determined by the two-tailed unpaired Student's *t* test. **P*<0.05; ****P*<0.001.

(B) Small intestinal sections of mice of the indicated genotypes at E18.5 were stained with anti-Reg3β or anti-Reg3γ antibodies (n=3 mice per each genotype). Scale bars, 100 μm. Results are representative of three independent experiments.

(C) Tissue extracts of the SI of mice of the indicated genotypes at E18.5 were analyzed by immunoblotting with the indicated antibodies (n=2 mice per each genotype). Each number indicates an individual mouse. Results are representative of two independent experiments.

(D) The expression of *Reg3b* and *Reg3g* mRNAs is abolished in the SI of mice on an *Il22*-/-, or *Rorc-gfp/gfp*, but not *Rag2*-/- background. mRNAs were prepared from the SI of 8- to 12-week-old mice of the indicated genotypes, and the expressions of *Reg3b* and *Reg3g* was determined by qPCR. Results are mean ± SEM (n= 4 to 12 per group). Statistical significance was determined by the two-tailed unpaired Student's t test. ***$P<0.001$; ns, not significant. (E) The expression of *Il22* mRNAs is abolished in the SI of *Rorc-gfp/gfp*, but not *Rag2*-/- mice. mRNAs were prepared as in (D), the expressions of *Il22* was determined by qPCR. Results are mean ± SEM (n= 4 to 12 per group). Statistical significance was determined by the two-tailed unpaired Student's t test. **$P<0.01$; ns, not significant.

ShindoFigS6

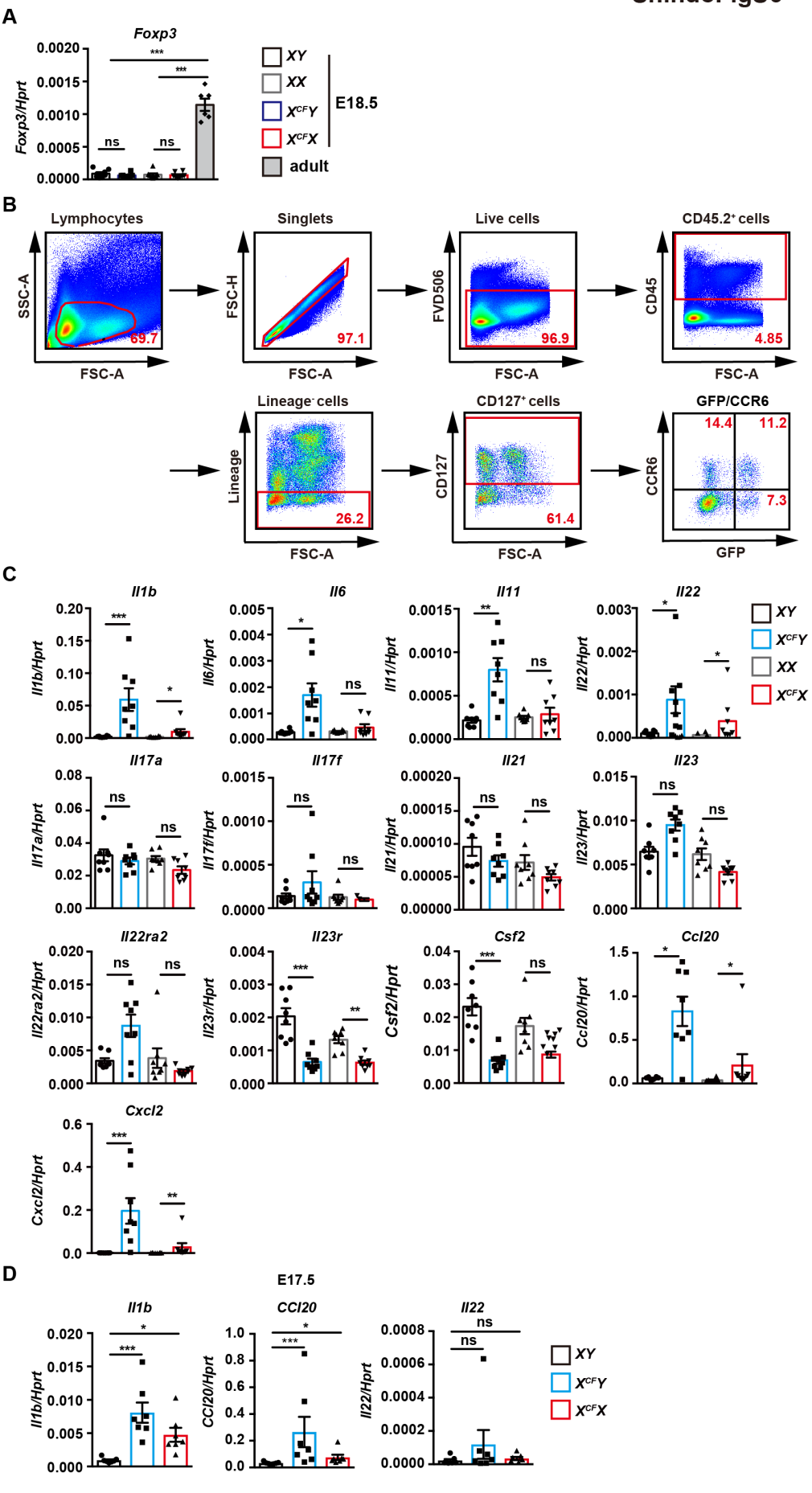

Figure S6. Gating strategy to analyze RORγt$^+$ ILCs and expression of ILC3 signature genes in the SI of *CFLARs* Tg mice, Related to Figure 5.

(A, C, D) RNAs were prepared from the SI of mice of the indicated genotypes at E18.5 (A, C) or E17.5 (D) or 8- to 12-week-old wild-type adult mice (A), and the expression of the indicated genes was determined by qPCR. Results are mean ± SEM (n=6 to 8 mice per each genotype). Statistical significance was determined by the two-tailed unpaired Student's *t* test. **P*<0.05; ***P*<0.01; ****P*<0.001; ns, not significant.

(B) Gating strategy of analysis of RORγt$^+$ ILC3s. Intestinal lamina propria cells were isolated as described in Transparent Methods. Live and CD45.2$^+$ cells were gated, and then lineage-negative cells were gated. CD127$^+$ cells were analyzed by the expression of GFP and CCR6. Representative results of three independent pooled experiments.

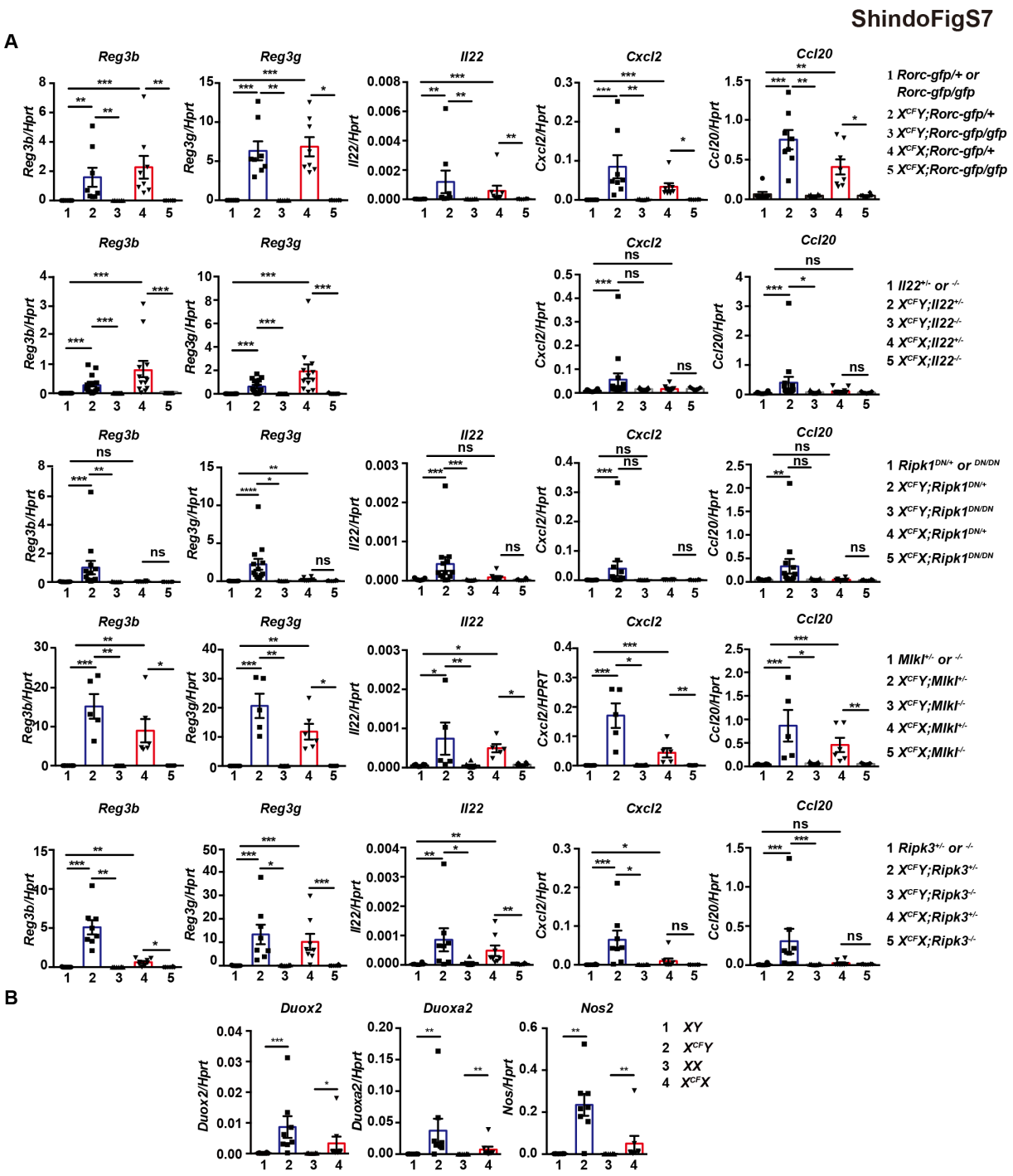

Figure S7. Deletion of genes associated with necroptosis, *Il22,* or *Rorc* downregulates the expression of various genes in the SI of *CFLARs* Tg mice, Related to Figure 6.

(A, B) mRNAs were prepared from the SI of mice of the indicated genotypes at E18.5, and the expression of the indicated genes was determined by qPCR. Results are mean ± SEM (n=5 to 15 mice per group). Statistical analysis was determined by the one-way ANOVA test (A) or the two-tailed unpaired Student's *t* test (B). **P*<0.05; ***P*<0.001; ****P*<0.001; ns, not significant.

Table S1. Upregulated genes in the SI of *CFLARs* Tg mice compared to wild-type mice, Related to Figure 5.

Accession No.	Symbol	Gene	Fold change
NM_011260	*Reg3g*	regenerating islet-derived 3 gamma	48.5
NM_011036	*Reg3b*	regenerating islet-derived 3 beta	35.1
NM_008204	*H2-M2*	histocompatibility 2, M region locus 2	21.4
NM_009140	*Cxcl2*	chemokine (C-X-C motif) ligand 2	21.1
NM_011315	*Saa3*	serum amyloid A 3	19.6
NM_0011685	*Pla2g4c*	phospholipase A2, group IVC (cytosolic, calcium-independent)	18.7
NM_008599	*Cxcl9*	chemokine (C-X-C motif) ligand 9	12.8
NM_010927	*Nos2*	nitric oxide synthase 2, inducible	11.6
NM_0011682	*Gsdmc2*	gasdermin C2	11.3
NM_177610	*Duox2*	dual oxidase 2	11.0
NM_028992	*Gsdmc4*	gasdermin C4	10.4
NM_173869|	*Stfa2l1*	stefin A2 like 1	10.3
NM_0011682	*Gsdmc2*	gasdermin C2	9.3
NM_016960|	*Ccl20*	chemokine (C-C motif) ligand 20	8.5
NM_008324	*Ido1*	indoleamine 2,3-dioxygenase 1	8.4
NM_0010825	*Stfa2*	stefin A2	8.3
NM_025777	*Duoxa2*	dual oxidase maturation factor 2	7.8
NM_010260	*Gbp2*	guanylate binding protein 2	7.6
NM_021274	*Cxcl10*	chemokine (C-X-C motif) ligand 10	7.3
NM_008147	*Gp49a*	glycoprotein 49 A	7.1
NM_011410	*Slfn4*	schlafen 4	6.9
NM_011337	*Ccl3*	chemokine (C-C motif) ligand 3	6.9
NM_011579|	*Tgtp1*	T-cell specific GTPase 1	6.7
NM_009114	*S100a9*	S100 calcium binding protein A9 (calgranulin B)	6.6
NM_0010825	*BC100530*	cDNA sequence BC100530	6.5
NM_009264	*Sprr1a*	small proline-rich protein 1A	6.5
NM_011579	*Tgtp1*	T-cell specific GTPase 1	6.4

NM_013650	*S100a8*	S100 calcium binding protein A8 (calgranulin A)	6.4
NM_144544	*2210407C*	RIKEN cDNA 2210407C18 gene	6.3
NM_0010014	*Tnip3*	TNFAIP3 interacting protein 3	5.8
NM_008361	*Il1b*	interleukin 1 beta	5.7
NM_013532	*Lilrb4*	leukocyte immunoglobulin-like receptor, subfamily B, member 4	5.6
NM_008392	*Irg1*	immunoresponsive gene 1	5.4
NM_009909	*Cxcr2*	chemokine (C-X-C motif) receptor 2	5.4
NM_010742	*Ly6d*	lymphocyte antigen 6 complex, locus D	5.3
NM_008530	*Ly6f*	lymphocyte antigen 6 complex, locus F	5.1
NM_011113	*Plaur*	plasminogen activator, urokinase receptor	5.0
NM_153564	*Gbp5*	guanylate binding protein 5	4.9
NM_0011462	*Iigp1*	interferon inducible GTPase 1	4.9
NM_010416	*Hemt1*	hematopoietic cell transcript 1	4.8
NM_0011360	*Anxa10*	annexin A10	4.7
NM_0011682	*Serpina3f*	serine (or cysteine) peptidase inhibitor, clade A, member 3F	4.7
NM_0010819	*Gm11428*	predicted gene 11428	4.7
NM_009903	*Cldn4*	claudin 4	4.7
NM_0010256	*Il1rl1*	interleukin 1 receptor-like 1	4.6
NM_009704	*Areg*	amphiregulin	4.6
NM_007607	*Car4*	carbonic anhydrase 4	4.6
NM_008620	*Gbp4*	guanylate binding protein 4	4.5
NM_010555	*Il1r2*	interleukin 1 receptor, type II	4.4
NM_008611	*Mmp8*	matrix metallopeptidase 8	4.4
NM_008491	*Lcn2*	lipocalin 2	4.3
NM_009252	*Serpina3n*	serine (or cysteine) peptidase inhibitor, clade A, member 3N	4.3
NM_0010332	*Nlrc5*	NLR family, CARD domain containing 5	4.1
NM_011452	*Serpinb9b*	serine (or cysteine) peptidase inhibitor, clade B, member 9b	4.1
NM_181596	*Retnlg*	resistin like gamma	4.1

RNAs were extracted from the SI of the indicated mice at E18.5 and analyzed using oligonucleotide arrays. Fold changed were calculated using the expression levels of each gene in the SI of *CFLARs* Tg mice compared to those of wild-type mice and top 55 genes are shown. Experiments were performed using two mice per each genotype and the average values of fold change are shown.

Table S2. **Primers used for qPCR in the study, Related to Figure 5.**

Ccl20:	5'- GCCTCTCGTACATACAGACGC-3'
	5'- CCAGTTCTGCTTTGGATCAGC-3'
Csf2:	5'- CTTTGAATGCAAAAAACCAGTCC-3'
	5'- TCCTGGCTCATTACGCAGGC-3'
Cxcl2:	5'- CCAACCACCAGGCTACAGG-3'
	5'- GCGTCACACTCAAGCTCTG-3'
Duox2:	5'- ACGCAGCTCTGTGTCAAAGGT-3'
	5'- TGATGAACGAGACTCGACAGC-3'
Duoxa2:	5'-GACGGGGTGCTACCCTTTTAC-3'
	5'-GCTAAGAAGGACTCTCACCAAC-3'
Foxp3:	5'-GGCGAAAGTGGCAGAGAGG-3'
	5'-AAGGCAGAG TCAGGAGAAGTTG-3'
Hprt:	5'- AACAAAGTCTGGCCTGTATCCAA -3'
	5'- GCAGTACAGCCCCAAAATGG-3'
Il1b:	5'- GCAACTGTTCCTGAACTCAACT-3'
	5'- ATCTTTTGGGGTCCGTCAACT-3'
Il6:	5'- GTATGAACAACGATGATGCACTTG-3'
	5'- ATGGTACTCCAGAAGACCAGAGGA-3'
Il11:	5'- CTGCACAGATGAGAGACAAATTCC-3'
	5'- GAAGCTGCAAAGATCCCAATG-3'
Il17a:	5'- CTGGAGGATAACACTGTGAGAGT-3'
	5'- TGCTGAATGGCGACGGAGTTC-3'
Il17f:	5'- CAAAACCAGGGCATTTCTGT-3'
	5'- ATGGTGCTGTCTTCCTGACC-3'
Il21:	5'- AGCCCCCAAGGGCCAGATCGC-3'
	5'- AGCTGCATGCTCACAGTGCCCCTTT-3'
Il22:	5'- TCCGAGGAGTCAGTGCTAAA-3'
	5'- AGAACGTCTTCCAGGGTGAA-3'
Il22ra2:	5'-TCAGCAGCAAAGACAGAAGAAAC-3'
	5'-GTGTCTCCAGCCCAACTCTCA-3'

Il23:	5’-GGGGAACATTATACTTTCCTGG-3’
	5’-CTAGATTCT GTTAGAACTGAGG-3’
Il23r:	5’-CCCAG ACAGTTTCCCAGGTTACAGC-3’
	5’-TGGCCAAGAAGACCATTCCCGACA-3’
Nos2:	5’-GTTCTCAGCCCAACAATACAAGA-3’
	5’-GTGGACGGGTCGATGTCAC-3’
Reg3b:	5’- CTCCTGCCTGATGCTCTTAT-3’
	5’- TTGTTACTC-CATTCCCATCC-3’
Reg3g:	5’- ACGAATCCTTCCTCTTCCTCAG-3’
	5’- GTCTTCACATTTGGGATCTTG-C-3’

Transparent Methods

Reagents

Murine TNF (34-8321, eBioscience), zVAD-fmk (3188-v, Peptide Institute), and Hoechst 33258 (Molecular Probes) were purchased from the indicated sources. The following antibodies were used in this study and were obtained from the indicated sources: anti-Reg3β (AF5110, R&D Systems, 1: 3000 for WB, 1: 200 for IHC), anti-cFLIP (Dave-2, Adipogen, 1: 500 for WB, 1: 200 for IF), anti-caspase-3 (9662, Cell Signaling, 1: 1000), anti-cleaved caspase-3 (9661, Cell Signaling, 1: 1000 for WB, 1: 200 for IHC or IF), anti-caspase-8 (1G12, Alexis, 1: 1000), anti-CCL20 (MAB7601, R&D SYSTEMS, 1: 200), anti-F4/80 (BM8, Caltag, 1: 100), anti-RIPK3 (IMG-5523-2, IMGENEX, 1: 3000), anti-phospho-RIPK3 (57220, Cell Signaling, 1: 1000 for WB, 1: 200 for IF), anti-tubulin (T5168, Sigma-Aldrich, 1: 40000), anti-STAT3 (sc-482, Santa-Cruz, 1: 1000), anti-phospho-STAT3 (9131, Cell Signaling, 1: 1000), anti-CD3 (Ab5690, Abcam, 1: 200) were purchased from the indicated sources. Anti-CD3 (145-2C11, 1: 200), anti-CD4 (RM4-5, 1: 200), anti-CD8 (53-6.7, 1: 200), anti-CD11b (M1/70, 1: 200), anti-CD11c (N418, 1: 200), anti-CD19 (1D3, 1: 200), anti-B220 (RA3-6B2, 1: 200), anti-Gr-1 (RB6-8C5, 1: 200), anti-Ly-6G (1A8, 1: 200), anti-CD45.2 (104, 1: 100), anti-TER-119 (TER-119, 1: 200), anti-CD127 (A7R34, 1: 200) antibodies were purchased from TONBO Biosciences. Anti-CCR6 antibody (140706, 1: 200) and Fixable Viability Dye eFluor 506 (65-0816-14) were purchased from BD and eBioscience. Anti-Reg3β (1: 1000) and anti-Reg3γ (1: 1000) antibodies were described previously (Matsumoto et al., 2012). HRP-conjugated donkey anti-rabbit IgG (NA934, 1:5000), HRP-conjugated sheep anti-mouse IgG (NA931, 1: 5000), HRP-conjugated goat anti-rat IgG (NA935, 1: 5000) antibodies were purchased from GE Healthcare Life Science. Alexa Fluor 594–conjugated donkey anti-rabbit IgG (A21207, 1: 500) and Alexa Fluor 488-conjugated donkey anti-goat IgG (A11055, 1: 500) antibodies were from Invitrogen. Biotin-conjugated goat anti-rabbit IgG (E0432, Dako, 1: 200), Biotin-conjugated rabbit anti-rat IgG (BA-4001, VECTOR, 1: 200) and biotin-conjugated rabbit anti-sheep IgG (BA-6000, VECTOR, 1: 200) antibodies, and HRP-conjugated streptavidin (P0397, Dako, 1: 300) were purchased from the indicated sources.

Cells

Primary MEFs were prepared from mice of the indicated genotypes at E14.5 after coitus using a standard method. MEFs below ten passages were used as primary MEFs for experiments. MEFs were maintained with DMEM containing 10% fetal calf serum.

Cell viability assay

MEFs were plated onto 96-well plates and cultured for 12 hours in DMEM containing 10% FCS. Then, cells were stimulated with the indicated concentrations of TNF in the absence or presence of zVAD-fmk

(20 μM) for 7 hours. Cell viability was determined by WST-1 (water soluble 2-(4-iodophenyl)-3-(4-nitrophenyl)-5-(2,4-disulfophenyl)[2H] tetrazolium monosodium salt-1) assay using a Cell Counting kit (343-07623, Dojindo).

Mice

Ripk3-/- (Newton et al., 2004) (provided by V. Dixit), *Mlkl*-/- (Dannappel et al., 2014) and *Ripk1*$^{DN/DN}$ (Polykratis et al., 2014) (provided by M. Pasparakis), *Il22*-/- (Zheng et al., 2008) (provided by Genentech, Inc.), and *Tnfrsf1a*-/- (Pfeffer et al., 1993) (provided by T.W. Mak) mice were described previously. *Rorc-gfp/gfp* mice (Eberl et al., 2004) were provided by K. Honda under the third party transfer agreement of the Jackson Lab. *Rag2*-/- mice (Hao and Rajewsky, 2001) were purchased from the Jackson Lab. C57/BL6 mice were purchased from Sankyo Lab. All experiments were performed according to the guidelines approved by the Institutional Animal experiments Committee of Kumamoto University, Juntendo University Graduate School of Medicine, Toho University School of Medicine, and Tokyo Medical University.

Generation of *CFLARs* Tg mice at the *Diap2* locus on the X-chromosome

We previously generated one ES cell line designated B210, in which a promoter trap vector was integrated into the *Diaphanous homolog 2 (Diap2)* gene on the X-chromosome (Taniwaki et al., 2005). We transfected a replacement vector for *CFLARs* where the expression of *CFLARs* was under the control of the *cytomegalovirus early enhancer/chicken b-actin (CAG)* promoter and flanked by two mutant *lox* sites into B210 cells (Figure 1A). The replacement vector was electroporated into B210 cells along with an expression vector for *Cre recombinase* to induce recombination between two mutant *lox* sites. Characterization of B210 ES cells harboring a gene trap vector at the *Diap2* locus on the X-chromosome will be published elsewhere. Selection was maintained for 5 days, and then colonies were picked into 48-well plates and expanded for freezing. The puromycin-resistant colonies were analyzed by Southern blotting and PCR to select ES cell lines showing successful integration of p*CAGGS-CFLARs*-pA. Positive clones were aggregated with ICR morula according to the protocol previously described. Germline transmission was obtained in three mouse lines, and two different lines were backcrossed onto C57BL/6N at least 5 generations. *CFLARs* Tg mouse lines, designated as C9 and C28, were used in this study.

Cre-ERT2 Tg mice were generated by an essentially similar to the protocol of generation of *CFLARs* Tg mice as described above. Detailed information of a vector of p*CAGGS-Cre-ERT2*-pA and characterization of *Cre-ERT2* Tg mice will be published elsewhere.

Western blotting

Murine tissues were homogenized with a Polytron (KINEMATICA) or cells were lysed in RIPA buffer [50 mM Tris-HCl (pH 8.0), 150 mM NaCl, 1% Nonidet P-40, 0.5% deoxycholate, 0.1% SDS, 25 mM β-glycerophosphate, 1 mM sodium orthovanadate, 1 mM sodium fluoride, 1 mM phenylmethylsulfonyl fluoride (PMSF), 1 μg/ml aprotinin, and 1 μg/ml leupeptin]. After centrifugation, tissue extracts or cell lysates were subjected to SDS polyacrylamide gel electrophoresis (SDS-PAGE) and transferred onto polyvinylidene difluoride (PVDF) membranes (Millipore). The membranes were analyzed with the indicated antibodies. The membranes were developed with Super Signal West Dura Extended Duration Substrate (Thermo Scientific) and analyzed with a LAS4000 or Amersham Imager 600 (GE Healthcare Life Sciences).

Histological, immunohistochemical, and immunofluorescence analyses

Murine tissues were fixed in 10% formalin and embedded in paraffin blocks. Paraffin-embedded tissue sections were used for hematoxylin and eosin (H&E) staining. TUNEL staining was performed with ApopTag Fluorescein *In Situ* Apoptosis Detection kit (S7110, Millipore) (for Figure 1G) or the *In Situ* Detection kit (Roche Diagnostics) (for Figure 2E). Briefly, paraffin-embedded sections were incubated with a TdT reaction mixture containing digoxigenin nucleotide and biotin-16-dUTP followed by incubation with fluorescein-conjugated anti-digoxigenin antibody and HRP–conjugated streptavidin, respectively. For immunostaining, paraffin-embedded sections were incubated with the indicated primary antibodies and then visualized with respective secondary antibodies. To detect cFLIPs, pRIPK3, Gr-1, and CCL20, the tyramide signal amplification (TSA) method was applied according to the manufacturer's instructions (NEL741001KT, PerkinElmer). Images were obtained by All In One analyzer (KEYENCE) or confocal microscopy (Nikon). Images were analyzed with KEYENCE software (KEYENCE) or NIS-Elements AR Analysis software (Nikon).

TEM analysis

Small intestines from mice of the indicated genotype at E17.5 or E18.5 were removed and fixed with 2% glutaraldehyde and 2% paraformaldehyde in 0.1 M phosphate buffer, pH 7.4. Slices of these fixed tissues were postfixed with 2% OsO_4, dehydrated in ethanol, and embedded in Epok 812 (Okenshoji Co.). Ultrathin sections were cut with an ultramicrotome (ultracut N or UC6: Leica), stained with uranyl acetate and lead citrate, and examined with a Hitachi HT7700 or JEOL JEM-1400 electron microscope.

Microarray analysis

We compared gene expression profiles of RNAs from the intestines of wild-type and *CFLARs* Tg mice at E18.5. Total RNAs were extracted from the small intestines of mice of the indicated genotype at E18.5 (n=2 mice per each genotype) using Sepasol-RNA I Super G according to the manufacturer's

instructions (09379-55, Nacalai Tesque), then labeled with Cy3. Samples were hybridized to a Mouse Oligonucleotide Microarray (G4121B, Agilent) according to the manufacturer's protocol. Arrays were scanned with a G2565BA Microarray Scanner System (Agilent). Data were analyzed using GeneSpring GX software (Agilent). The accession number for the microarray data reported in this paper is NCBI GEO: GSE120982.

Heat maps and principal component analysis plots were generated in the R-method. Gene Ontology (GO) enrichment analysis was performed using the ToppGene Suite (http://toppgene.cchmc.org/)(Chen et al., 2009).

Quantitative polymerase chain reaction assays

Total RNAs were extracted with the small intestines of mice of the indicated genotype at E18.5 and cDNAs were synthesized with the Revertra Ace qPCR RT Kit (Toyobo). Quantitative polymerase chain reaction (qPCR) analysis was performed with the 7500 Real-Time PCR detection system with CYBR green method of the target genes together with an endogenous control, murine *Hprt* with 7500 SDS software (Applied Biosystems). The primers used for qPCR were listed in Table S2.

Flow cytometry

After genotyping, three to four small intestines of the fetus of the same genotype at E18.5 were pooled and cut into small fragments and then digested with 1 mg/ml of collagenase (032-22364, Wako) in 10% FCS RPMI at RT for 30 min. Cells were passed through a 70 μm cell strainer, and single cell suspension was prepared. Cells were incubated with the indicated antibodies for 30 min. Fixable Viability Dye eFluor 506 (65-0816-14, eBioscience) was used to distinguish live cells from dead cells, and live cells were analyzed with the indicated antibodies.

Gating strategy for RORγt$^+$ ILC3s analysis was shown in Figure S6B. Briefly, CD45.2-positive but all lineage markers-negative cells were gated, and GFP-positive cells were analyzed by the expression of CCR6. The lineage markers used here were CD3, CD19, CD11b, CD11c, Gr-1, and TER-119. Data were obtained on a Fortessa (GE Healthcare) and analyzed by a Flow-Jo software (GE Healthcare).

Statistical analysis

Statistical analysis was performed by the two-tailed unpaired Student's *t* test or the one-way ANOVA test. $P < 0.05$ was considered to be statistically significant.

Supplemental References

Chen, J., Bardes, E.E., Aronow, B.J., and Jegga, A.G. (2009). ToppGene Suite for gene list enrichment analysis and candidate gene prioritization. Nucleic Acids Res *37*, W305-311.

Dannappel, M., Vlantis, K., Kumari, S., Polykratis, A., Kim, C., Wachsmuth, L., Eftychi, C., Lin, J., Corona, T., Hermance, N.*, et al.* (2014). RIPK1 maintains epithelial homeostasis by inhibiting apoptosis and necroptosis. Nature *513*, 90-94.

Eberl, G., Marmon, S., Sunshine, M.J., Rennert, P.D., Choi, Y., and Littman, D.R. (2004). An essential function for the nuclear receptor RORgamma(t) in the generation of fetal lymphoid tissue inducer cells. Nat Immunol *5*, 64-73.

Hao, Z., and Rajewsky, K. (2001). Homeostasis of peripheral B cells in the absence of B cell influx from the bone marrow. J Exp Med *194*, 1151-1164.

Matsumoto, S., Konishi, H., Maeda, R., Kiryu-Seo, S., and Kiyama, H. (2012). Expression analysis of the regenerating gene (Reg) family members Reg-IIIbeta and Reg-IIIgamma in the mouse during development. J Comp Neurol *520*, 479-494.

Newton, K., Sun, X., and Dixit, V.M. (2004). Kinase RIP3 is dispensable for normal NF-kappa Bs, signaling by the B-cell and T-cell receptors, tumor necrosis factor receptor 1, and Toll-like receptors 2 and 4. Mol Cell Biol *24*, 1464-1469.

Pfeffer, K., Matsuyama, T., Kundig, T.M., Wakeham, A., Kishihara, K., Shahinian, A., Wiegmann, K., Ohashi, P.S., Kronke, M., and Mak, T.W. (1993). Mice deficient for the 55 kd tumor necrosis factor receptor are resistant to endotoxic shock, yet succumb to L. monocytogenes infection. Cell *73*, 457-467.

Polykratis, A., Hermance, N., Zelic, M., Roderick, J., Kim, C., Van, T.M., Lee, T.H., Chan, F.K.M., Pasparakis, M., and Kelliher, M.A. (2014). Cutting edge: RIPK1 Kinase inactive mice are viable and protected from TNF-induced necroptosis in vivo. J Immunol *193*, 1539-1543.

Taniwaki, T., Haruna, K., Nakamura, H., Sekimoto, T., Oike, Y., Imaizumi, T., Saito, F., Muta, M., Soejima, Y., Utoh, A.*, et al.* (2005). Characterization of an exchangeable gene trap using pU-17 carrying a stop codon-beta geo cassette. Dev Growth Differ *47*, 163-172.

Zheng, Y., Valdez, P.A., Danilenko, D.M., Hu, Y., Sa, S.M., Gong, Q., Abbas, A.R., Modrusan, Z., Ghilardi, N., de Sauvage, F.J.*, et al.* (2008). Interleukin-22 mediates early host defense against attaching and effacing bacterial pathogens. Nat Med *14*, 282-289.